Effect of in-plane alignment on selective area grown homo-epitaxial nanowires

Nagda, G; Beznasyuk, D V; Nygard, J; Jespersen, T S

Published in:
Nanotechnology

Link to article, DOI:
10.1088/1361-6528/acca27

Publication date:
2023

Document Version
Publisher's PDF, also known as Version of record

Effect of in-plane alignment on selective area grown homo-epitaxial nanowires

OPEN ACCESS
IOP Publishing
Nanotechnology
Nanotechnology **34** (2023) 275702 (7pp)
https://doi.org/10.1088/1361-6528/acca27

Effect of in-plane alignment on selective area grown homo-epitaxial nanowires

G Nagda[1], D V Beznasyuk[1,2], J Nygård[1] and T S Jespersen[1,2]

[1] Center for Quantum Devices, Niels Bohr Institute, University of Copenhagen, 2100 Copenhagen, Denmark
[2] Department of Energy Conversion and Storage, Technical University of Denmark, 2800 Kgs. Lyngby, Denmark

E-mail: gunjan.nagda@nbi.ku.dk

Received 1 February 2023, revised 24 March 2023
Accepted for publication 4 April 2023
Published 21 April 2023

Abstract

In-plane selective area growth (SAG) of III–V nanowires (NWs) has emerged as a scalable materials platform for quantum electronics and photonics applications. Most applications impose strict requirements on the material characteristics which makes optimization of the crystal quality vital. Alignment of in-plane SAG NWs with respect to the substrate symmetry is of importance due to the large substrate-NW interface as well as to obtain nanostructures with well-defined facets. Understanding the role of mis-orientation is thus important for designing devices and interpretation of electrical performance of devices. Here we study the effect of mis-orientation on morphology of selectively grown NWs oriented along the [1 $\bar{1}$ $\bar{1}$] direction on GaAs(2 1 1)B. Atomic force microscopy is performed to extract facet roughness as a measure of structural quality. Further, we evaluate the dependence of material incorporation in NWs on the orientation and present the facet evolution in between two high symmetry in-plane orientations. By investigating the length dependence of NW morphology, we find that the morphology of $\approx$1 μm long nominally aligned NWs remains unaffected by the unintentional misalignment associated with the processing and alignment of the sample under study. Finally, we show that using Sb as a surfactant during growth improves root-mean-square facet roughness for large misalignment but does not lower it for nominally aligned NWs.

Supplementary material for this article is available online

Keywords: selective area growth, GaAs nanowires, molecular beam epitaxy, semiconductor nanowires, AFM characterization, in-plane orientation, substrate fabrication

(Some figures may appear in colour only in the online journal)

1. Introduction

Selective area growth (SAG) of III–V materials is a flexible and potentially scalable method for obtaining deterministic and reproducible in-plane nanowires (NWs) as a platform for NW technologies [1]. SAG using molecular beam epitaxy (MBE), typically defined by lithographic techniques, allows precise control of the position and size of NWs and the creation of large scale arrays and networks of high quality. Unlike conventional metal catalyzed, out-of-plane vapour–liquid–solid or vapour–solid growth, the SAG approach obviates time consuming and uncontrolled pick-and-place steps in device fabrication and enables large scale integration of nanostructures into complex device geometries [2].

The structural quality of SAG nanostructures depends on the substrate orientation [3], substrate fabrication methods, lattice mismatch between the substrate and the grown material [4], pre-growth substrate annealing methods [4], and the thermodynamics and kinetics during crystal growth [5]. SAG using MBE of semiconductors such as Si has already been reported

four decades ago [6] and for GaAs SAG, facet formation and evolution on GaAs(0 1 1) [7, 8] has been studied and various models of growth mechanisms have been proposed [5–9, 11]. SAG of InAs NWs [3] and nanostructures [12] on InP substrates using chemical beam epitaxy has been reported, demonstrating different cross-sectional shapes and facets dependent on the substrate symmetry and growth parameters. InAs SAG NWs grown on GaAs(Sb) [2] and/or InGaAs [4] buffer layers showed an enhanced crystal quality and improved electron mobility as compared to non-optimized crystals. However, formation of homogeneous group-III alloys still remains a challenge owing to facet dependent incorporation [13] and differing behaviour of group-III elements on the dielectric mask [5]. Moreover, the scalability of SAG comes with the price of NWs being epitaxially connected to the substrate along the entire length. This makes the crystals highly sensitive to interface and surface quality and this remains a challenge compared to out-of-plane NW growth.

In addition, the SAG NW becomes sensitive to mis-orientation between the NW axis and the high symmetry directions of the substrate which is unavoidable due to the tolerance of substrate manufacturing and fabrication methods. Although such tolerance and mis-orientation is small, its effect is amplified in growth of long SAG NWs due to the epitaxial registry between NW and substrate. So far, however, the resulting consequences for structural disorder have not been addressed.

Here we present a systematic study of the effect of mis-orientation on MBE grown homoepitaxial GaAs and surfactant mediated GaAs(Sb) SAG NWs on GaAs(2 1 1)B. Increasing mis-orientation leads to increasing formation of discrete crystal steps on the NW facets. Although the correlation of structural disorder with the electrical characteristics have not yet been quantified for SAG NWs, nanoscale changes in faceting of NWs have been shown to modify the current density in NW devices [14]. Additionally, growth of subsequent transport-active InGaAs and InAs layers on such imperfect NWs will likely result in strain inhomogeneity locally within the crystal which has been reported to have a direct effect on the resistivity [15].

We investigate [1 $\bar{1}$ $\bar{1}$] oriented NWs, which exhibit a symmetric cross-section bound by {1 1 0} facets, to study the influence of mis-orientation and quantify the structural morphology of the NW in terms of facet roughness (S_q). Information about material incorporation in SAG NWs is obtained by studying the volume dependence of the NWs on the in-plane orientation. Changing cross-sectional shapes of the NWs oriented between high-symmetry in-plane orientations provides information about the facet evolution. We also demonstrate the effect of NW length on the morphology and show that for a given mis-orientation, there is a length scale for which the discontinuities in the NW facets are minimized. We find that as previously reported for standard (1 0 0) substrates [2], Sb also has a surfactant effect during GaAs growth on the (2 1 1)B orientation. A smoother NW surface can be achieved for largely misaligned NWs, however, it has a negligible effect at small misalignment. Such information may be used for directing design of e.g. electrical devices sensitive to crystal imperfections.

2. Experimental methods

The steps involved in substrate fabrication for SAG are shown in figure 1(a): first, 10 nm of SiO_2 is deposited onto a GaAs(2 1 1) B substrate using plasma enhanced chemical vapour deposition. After spin coating 300 nm of CSAR13 resist [16], electron beam lithography is used to expose regions on the SiO_2 mask which are then etched using an inductively coupled plasma of a mixture of tetrafluoromethane (CF_4) and molecular hydrogen (H_2) thereby exposing the GaAs substrate. The SAG mask design used in this study consists of rectangles with length $L_{NW} = 1$–$6\ \mu$m and width $W_{NW} = 150$ nm in the [1 $\bar{1}$ $\bar{1}$] and [0 1 $\bar{1}$] directions respectively ($\theta = 0°$) and with varying misalignment from that direction to cover all in-plane directions in steps of 3°. The resist is removed using standard cleaning procedures and the substrate is thoroughly cleaned using O_2 plasma before transfer to the MBE chamber. Prior to growth, the substrate is thermally annealed twice: at 400 °C in the transfer module for 60 min to remove organic contaminants, and at 620 °C under As_4 over-pressure in the growth chamber for 18 min to remove the native oxide from the GaAs surface.

Using a previously established range of parameters ensuring growth on the exposed GaAs substrate without parasitic growth on the SiO_2 mask [17], we grow GaAs and GaAs(Sb) NWs at a substrate temperature of $T_{sub} = 600$ °C and a Ga growth rate of 0.1 ML s^{-1} for 30 min corresponding to ≈50 nm of planar GaAs growth on a GaAs(1 0 0) substrate. An As/Ga ratio of 9 and Sb/Ga ratio of 3 is used for GaAs and GaAs(Sb) growths, respectively, ensuring growth rates determined by the Ga flux. The influence of the substrate orientation on the selectivity window is not significant at these conditions and parasitic growth is not observed (see supplementary section S1).

For this study, a GaAs(Sb) substrate with a diameter of 2 inches was processed with identical patterns repeated on four quarters. The pattern consists of NW openings with different lengths and angles. Following the fabrication, the wafer was cleaved into quarters and two samples were grown; one with GaAs and one with GaAs(Sb). The samples thus have the same fabrication-related tolerances, and the resulting [1 $\bar{1}$ $\bar{1}$]-oriented NWs were systematically characterized using scanning electron microscopy (SEM) and atomic force microscopy (AFM). Individual steps on the NW facets were identified by performing AFM along the NW. Details of the AFM operating parameters are included in supplementary section S2.

3. Results and discussion

3.1. Origin of SAG NW misalignment

SAG is lithographically defined, making it technically possible to define a template with a very large degree of flexibility and along any direction. It is therefore important to understand the influence of substrate symmetry for the resulting crystal growth. Further, as discussed below, the tolerances of materials and processes lead to some degree of

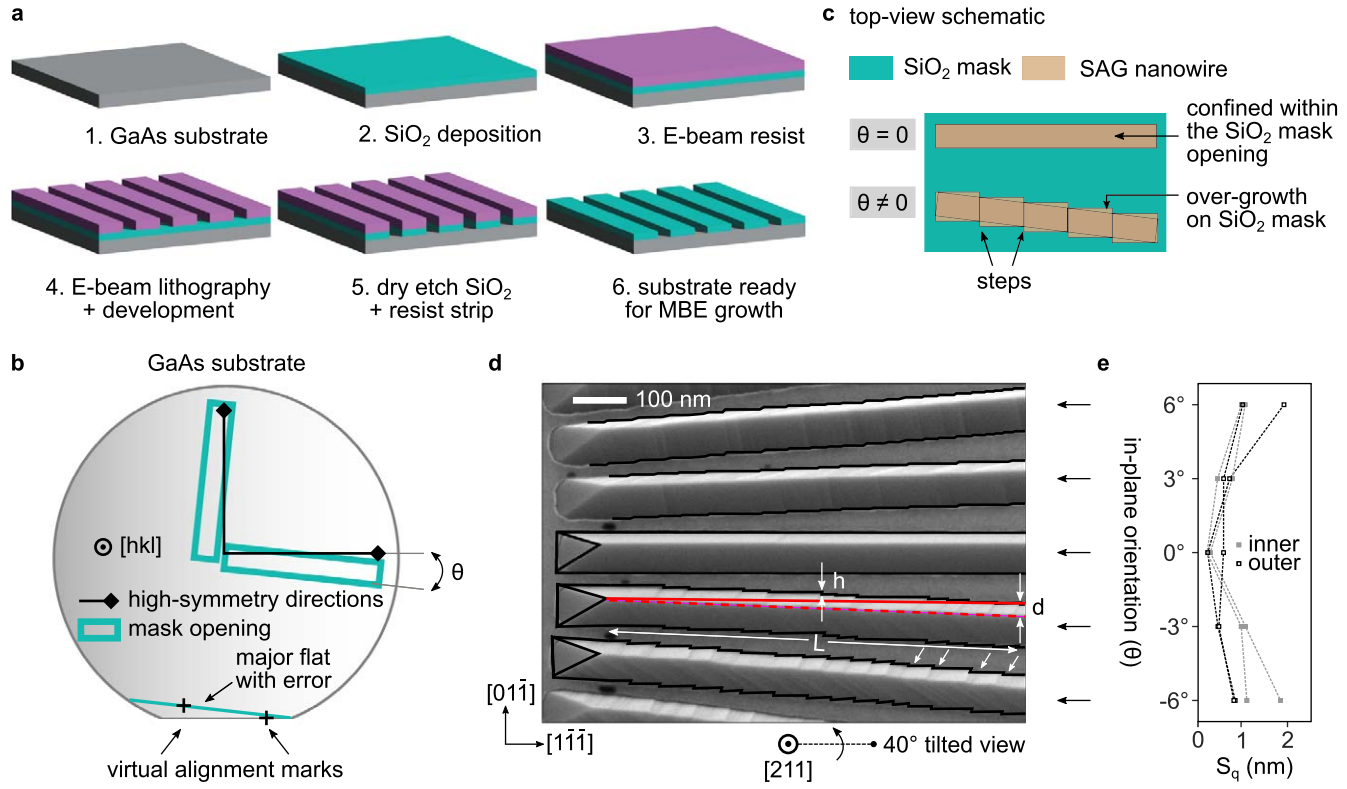

Figure 1. Effect of in-plane and out-of-plane mis-orientation on SAG NWs. (a) Schematic of the steps involved in substrate fabrication for SAG. (b) Top-view schematic of a substrate indicating typical errors in out-of-plane orientation (color gradient) and the orientation of the major flat (green line) along with the co-ordinate system used for lithographic processes. (c) Top-view schematic of SAG NWs that are aligned (no steps) and misaligned (with steps) with respect to a high-symmetry in-plane orientation. (d) a 40°-tilted SEM image of a series of GaAs(Sb) NWs oriented along the [1 $\bar{1}$ $\bar{1}$] direction and in increments of 3° on GaAs(2 1 1)B. The overlaid schematic highlights the geometric parameters relevant for calculating the angle of mis-orientation. **e** Facet roughness S_q for the inner (outer) NW facets facing toward (away from) the [1 $\bar{1}$ $\bar{1}$]-oriented NW as a function of in-plane orientation.

uncertainty in aligning SAG patterns to the symmetry of the substrate and the consequences need to be addressed.

A typical GaAs substrate received from the manufacturer comes with a margin of error with respect to the specified out-of-plane (substrate surface) and in-plane (major flat) orientations. This is illustrated in the top-view schematic in figure 1(b) where the the color gradient depicts a hypothetical error in the out-of-plane orientation relative to the specifications (ϕ) from left to right and the green line illustrates the supplied major flat which is mis-oriented by an angle θ with respect to the actual crystal direction. An out-of-plane mis-orientation ($\phi \neq 0$) leads to step edges on the surface. While this is beneficial for planar growth since it promotes the layer-like growth [18], it might also lead to height variations in NWs grown in-plane. However, for the dimensions of NWs considered in this study, the height of GaAs(Sb) NWs (taken along the top facet) remains constant along a length of $L_{NW} = 4\ \mu$m (see supplementary section S3). Thus, out-of-plane mis-orientation is not considered for the remainder of the analysis.

For SAG NWs used in this study, the trench openings in the SiO_2 mask impose a constraint on the growth dynamics that are nanoscale in one dimension (trench width) and several microns long in the other (trench length). The NW facets that develop during growth are dependent on the orientation of the trench openings along the length (see details about NW faceting in supplementary section S4). In-plane misalignment of the trench openings for NW growth is caused by external misalignment due to manufacturing errors during wafer flat grinding and internal misalignment due to the tolerance of lithographic procedures. The external misalignment for the substrates used in this study as provided by the manufacturer is maximally $\pm 0.1°$. Assuming that errors in stage movement during electron beam lithography due to thermal drift and precision of the tool itself are negligible, the major contribution to internal misalignment still comes from the error in determining the edge of the major flat which is used to align the mask design with virtual alignment marks with respect to the major flat (see figure 1(b)). This is because the flat grinding and polishing processes will not result in atomically flat edges and surfaces [19] leading to ambiguity in placement of the alignment marks. We estimate the maximal error in determining the major flat edge, as a result of rounded edges of the substrate, to be $\pm 0.4°$. Typically, the substrates from the same manufacturing batch will have the same external error and the varying internal error in between different lithographic runs and the total misalignment will be the combined result of both, i.e. $\pm 0.5°$. The resulting trench openings will thus be misaligned with respect to the high symmetry in-plane directions.

Due to the epitaxial connection between the substrate and the SAG NW, misalignment of the NW results in sections of the NW to overgrow on the SiO_2 mask, in order to maintain the NW facets with low surface energy. Since the crystal does not grow epitaxially on the SiO_2 mask, the overgrowth occurs in segments, as illustrated in the top-view schematic in figure 1(c) of a perfectly aligned NW and one that has a misalignment with respect to the high-symmetry in-plane direction. The distance at which it becomes energetically unfavourable for crystal growth on the mask, the NW facet forms a step towards the trench axis and this repeats along the NW length. Figure 1(d) shows a 40°-tilted SEM image of GaAs(Sb) NWs on GaAs(2 1 1)B. The middle NW is nominally aligned along the [1 $\bar{1}$ $\bar{1}$] direction and bound by {1 1 0}-type facets. The surrounding NWs are oriented along $\theta = \pm 3°, \pm 6°$. The NWs aligned at 3° and 6° show growth in segments separated by steps on the inclined facets (indicated by arrows, and emphasized by the black outline) and these segments become shorter with increasing mis-orientation. In the following, we consider a NW segment of length L (excluding the end facets), where the step-height along the facet is denoted as h and number of steps as n (figure 1(d)). The angle of mis-orientation θ for a NW can be deduced using geometry: $\theta = \tan^{-1}\left(\frac{d}{L}\right)$ where the total step displacement, $d = h' \times n$, where h' is the projection of h onto the substrate plane. The parameters n and h were determined through careful analysis of high-resolution AFM topographic maps as discussed in detail in supplementary section S5. Using this we obtain $\theta = 0.26° \pm 0.04°$ for the misalignment of the nominally [1 $\bar{1}$ $\bar{1}$]-oriented NW from the real [1 $\bar{1}$ $\bar{1}$] direction of the substrate. Here the error is due to the accuracy of $\Delta d = 2$ nm in measuring the total step displacement. The value for θ is thus consistent with the tolerances of experimentally determining the in-plane orientation of the substrate.

The step density on the NWs facets is also quantified as the root mean square facet roughness (S_q), which is extracted using AFM. Figure 1(e) depicts S_q for the inner (outer) NW facets facing toward (away from) the [1 $\bar{1}$ $\bar{1}$]-oriented NW as a function of in-plane orientation. Increasing number of steps with increasing mis-orientation results in a larger S_q and is minimized for the nominally [1 $\bar{1}$ $\bar{1}$]-oriented NW. We propose two ways to minimize S_q: finding the length scale for which NWs can grow step-free despite an in-plane misalignment and secondly, the use of Sb as a surfactant during GaAs growth to suppress step formation. However, we first examine how in-plane orientation affects material incorporation and facet evolution of GaAs(Sb) NWs grown on GaAs(2 1 1)B.

3.2. Material incorporation and facet evolution

Electrical characteristics of SAG NWs have been known to depend on the structural characteristics such as NW and facet orientations [3]. The faceting of NWs depends on the substrate symmetry and growth conditions and in turn also affects the growth dynamics. Thus, we investigate how the in-plane orientation affects the material incorporation in NWs. For this, we perform AFM on 120 NWs that are positioned in a circular array such that NWs along $\theta = 0°, 90°, 180°$ and 270° correspond to [1 $\bar{1}$ $\bar{1}$], [0 1 $\bar{1}$], [$\bar{1}$ 1 1] and [0 $\bar{1}$ 1] respectively. Figure 2(a) shows a polar plot of the NW volume normalized to the smallest volume, V_0 (corresponding to the [1 $\bar{1}$ $\bar{1}$]-oriented NW) as a function of angle. All 120 NWs are included in a single $17 \times 17\ \mu m^2$ scan. To check for artifacts due to the AFM scan direction, the measurement was performed parallel to [1 $\bar{1}$ $\bar{1}$] and [0 1 $\bar{1}$] directions. Scan parameters and the method for volume extraction is presented in supplementary sections S2 and S6, respectively.

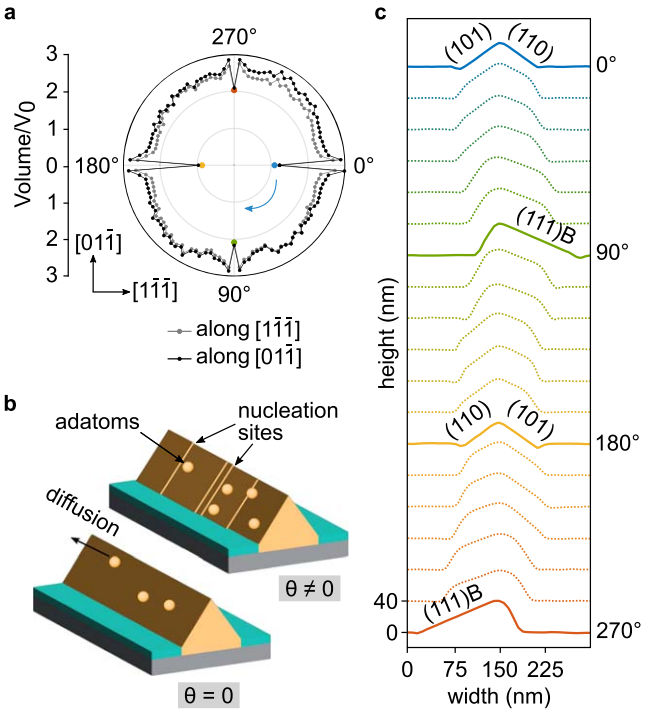

Figure 2. Material incorporation in NWs oriented along different in-plane directions. (a) Polar plot depicting the individual NW volume of 120 GaAs(Sb) NWs grown on GaAs(2 1 1)B normalized to the volume of a [1 $\bar{1}$ $\bar{1}$]-oriented nanowire, as a function of in-plane orientation. (b) Schematic of a NW aligned (smooth facets) and misaligned (facets with steps) with respect to a high-symmetry in-plane direction. (c) Waterfall plot of cross-sectional profiles of NWs that are oriented 15° apart. The dominant facets are as labelled and the profiles are color coded to their respective normalized volumes in (a) and are extracted along the direction of the blue arrow in (a).

As seen in figure 2(a), the NW volumes extracted from both scan directions follow a similar trend. The volume is significantly smaller for NWs oriented along the high-symmetry orientations. With increasing mis-orientation, the NWs exhibit increasing step density (as seen in figure 1(d)). Since nucleation at step edges minimises the surface free energy by incorporation of additional adatoms within the growing crystal [20], these NWs incorporate more material as each step acts as a nucleation site for incoming adatoms (see schematic in figure 2(b)). The activation energy for diffusion and desorption is higher at a nucleation site, thus increasing the probability that adatoms will instead accumulate and nucleate. This is consistent with the dramatic increase in volume of misaligned NWs as seen in figure 2(a).

Furthermore, the neighboring NWs experience an increased flux due to the expelled adatoms from the aligned NWs. This further increases the volume of the NWs next to the aligned NWs and may explain the small decay for further mis-oriented NWs. Figure 2(a) also shows that the [1 $\bar{1}$ $\bar{1}$]-oriented NWs incorporate less material compared to the [0 1 $\bar{1}$]-oriented NWs. This can be attributed to a longer Ga adatom diffusion length along the ⟨111⟩ direction [21] which causes a fraction of the incoming adatoms to diffuse along the NW length and be expelled onto the SiO_2 mask in the early stages of NW growth where the {1 1 0} facets have not developed yet. As the NW grows with increasing time and starts developing facets, the resulting material incorporation is a combined result of the adatom diffusion length along the ⟨111⟩ direction (NW axis) as well as the {1 1 0} facets of the NW (facets labelled in figure 2(c)).

To visualize the facet transformation of the NWs dependent on the in-plane orientation in this study, we extract an AFM topographical profile across the approximate center of the length of the NWs spaced 15° apart, starting from the [1 $\bar{1}$ $\bar{1}$]-oriented NW (figure 2(c)). The blue arrow in figure 2(c) corresponds to the direction along which the profiles were extracted. NWs oriented along high-symmetry directions exhibit well defined facets dictated by Wulff construction [22] thereby minimising the surface free energy of the crystal. The mis-oriented NWs exhibit a mixture of different facets along with increased material incorporation. Note that the (1 1 1)B facet tends to develop for NWs already at ≈15° deviations from the [1 $\bar{1}$ $\bar{1}$]-oriented NWs despite having a higher surface free energy as compared to the (0 1 1) facet for pure GaAs [23]. This can be attributed to the surfactant effect of Sb during GaAs growth [24]. The development of different facets along with differing adatom diffusion length and density of nucleation sites further complicates the interpretation of material incorporation within the mis-oriented NWs.

3.3. Effect of NW length

For a given substrate after a fabrication run for SAG, since the error in defining the NW trenches is fixed, the resulting step density on the NW facets must also be constant. However, the free surface at the ends of the trench may allow for a larger degree of overgrowth on the SiO_2 mask, thus allowing for a larger tolerance towards misalignment. Thus, to find the length scale for which it is possible to obtain a NW with smooth facets without steps, nominally [1 $\bar{1}$ $\bar{1}$]-oriented GaAs (Sb) NWs with $L_{NW} = 1$–$6\ \mu$m and $W_{NW} = 150$ nm were grown (AFM topography of the NWs is presented in supplementary section S7). AFM was performed on a total of 16 NWs and the corresponding n on both facets are tabulated in figure 3(b). As expected, we find that the number of steps on the NWs is linearly dependent on the NW length and the resulting dependence of n along both NW facets is presented in figure 3(a). However, performing a linear fit on the n dependence averaged for both facets, we find that it does not extrapolate to zero at $L = 0\ \mu$m but instead at a finite length L^*. Thus for NWs shorter than L^*, NWs exhibit no steps. To

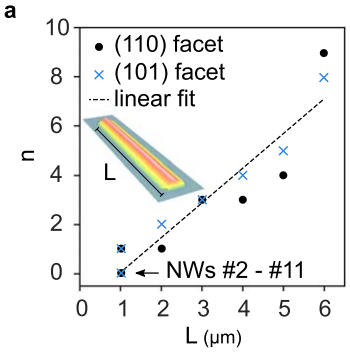

NW #	L (μm)	$n_{(110)}$	$n_{(101)}$
1	1	1	1
2	1	0	0
3 ⋮ 11	1 ⋮ 1	0 ⋮ 0	0 ⋮ 0
12	2	1	2
13	3	3	3
14	4	3	4
15	5	4	5
16	6	9	8

Figure 3. Length dependence of number of steps along NW facets (a) Number of steps (n) as a function of NW length (L). A linear fit is performed and extrapolated to obtain a length L^* for which NWs with no steps can be obtained. (b) A list of NWs with different L and the corresponding n on either facets. 10 out of 11 1 μm long NWs exhibit no steps.

eliminate the possibility of a statistical anomaly, AFM was performed on multiple NWs for $L_{NW} = 1\ \mu$m, where 10 out of 11 NWs show no steps at all. Performing a linear fit on the n dependence including all 16 NWs, we obtain $L^* = 0.96 \pm 0.18\ \mu$m. The slope of the fit gives us a step density in the middle of an arbitrarily long NW to be $1.41 \pm 0.07\ \mu m^{-1}$. The value of L^* depends on the mis-orientation-$\theta = 0.26° \pm 0.04°$ in the present case - and is thus specific to the sample and fabrication run. This is also consistent with our findings shown in supplementary section S8, where ends of the NWs oriented at an angle of ±3° and ±6° away from the nominally [1 $\bar{1}$ $\bar{1}$]-oriented NW show a tendency to overgrow more on the SiO_2 mask with few to no steps and gradually change the orientation towards the [1 $\bar{1}$ $\bar{1}$] direction.

It should be emphasized that the quantitative results obtained here can be extended towards homoepitaxial growth of NWs on both conventional and novel substrate orientations. Each substrate fabricated for SAG can be characterized post-growth to estimate the collective internal and external error in defining the NW trenches and the resulting length scale for which step-free NWs can be obtained. For experiments wherein longer SAG NWs are necessary by design, AFM characterization can be performed prior to device fabrication in order to place electrical contacts in segments of the NWs that exhibit no steps along the facets. Thus, even though we cannot completely eliminate the morphological imperfection in the NWs, careful design of the experiment can lead to minimized contribution from high S_q.

3.4. Sb as surfactant

Finally, we consider the use of Sb as a surfactant for reducing S_q. GaAs NWs were grown on GaAs(2 1 1)B with and without Sb and also with varying degrees of misalignment with respect to the [1 $\bar{1}$ $\bar{1}$] direction. The resulting 3D AFM topography for both GaAs and GaAs(Sb) NWs are shown in figures 4(a) and (b), respectively. Again, the number of steps on NW facets clearly increases with mis-orientation (arrows in figures 4(a) and (b)), and the effect is more pronounced for

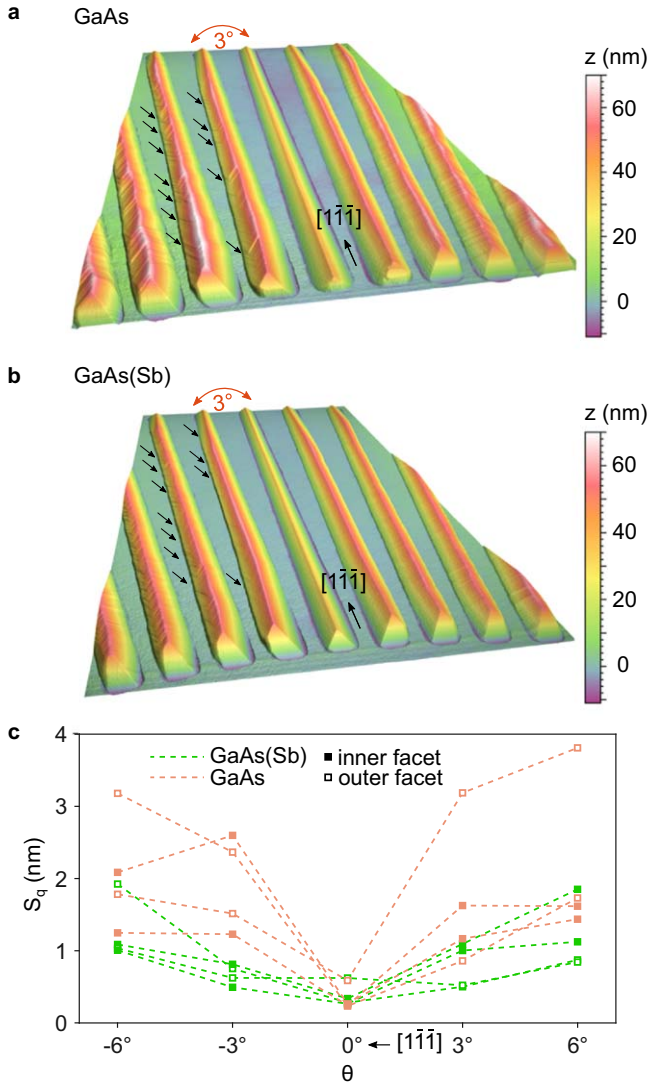

Figure 4. Effect of Sb as a surfactant on the NW morphology. Series of (a) GaAs and (b) GaAs(Sb) NWs on GaAs(2 1 1)B oriented along the [1 $\bar{1}$ $\bar{1}$] direction as well as NWs oriented in increments of 3° with respect to it. (c) Dependence of S_q on in-plane orientation for GaAs and GaAs(Sb) NWs. S_q is also presented for the inner (outer) facet of the misaligned NWs facing toward (away from) the [1 $\bar{1}$ $\bar{1}$]-oriented NW.

GaAs NWs compared to the GaAs(Sb) NWs. The corresponding dependence of S_q is shown in figure 4(c) for inner (outer) facet facing toward (away from) the [1 $\bar{1}$ $\bar{1}$]-oriented NW. These facets exhibit different step edges due to different in-plane polarity on the substrate (for details see supplementary section S9). Sb reduces S_q for $\theta \neq 0$ and thus helps reducing the effect of mis-orientation. The lowest value of $S_q \approx 0.4$ nm is observed for both nominally [1 $\bar{1}$ $\bar{1}$]-oriented GaAs and GaAs(Sb) NWs and is comparable to that of a substrate prior to any fabrication processing. Thus, based on the two samples we investigated for the case of [1 $\bar{1}$ $\bar{1}$]-oriented GaAs NWs on GaAs(211)B, we find that Sb does not improve the crystal quality as opposed to GaAs(Sb) SAG NWs grown under similar conditions on conventional GaAs(1 0 0) substrates [2, 4, 5].

Surfactants are known to modify surface free energies and adatom diffusion lengths for compound semiconductors and have been employed to suppress 3D island growth [24, 25]. Despite the possible surfactant effect of locally changing the facets surface free energy during crystal growth, there is no impact on the overall cross-sectional shape of the nominally [1 $\bar{1}$ $\bar{1}$]-oriented NWs shown in figure 4. The use of Sb as a surfactant for in-plane homoepitaxial GaAs growth on GaAs(1 0 0) substrates has been reported to demonstrate a reduction in S_q [2]. A similar effect in suppression of S_q is observed in this study for largely misaligned [1 $\bar{1}$ $\bar{1}$]-oriented NWs grown on a GaAs(2 1 1)B substrate and confirms the feasibility of the method for achieving smoother facets. However, as demonstrated in the previous section, it does not guarantee NWs devoid of steps above $L_{\mathrm{NW}} \approx 1\,\mu$m. We conclude that using the NW length is a promising way to ensure minimal contribution to morphological disorder in this case.

4. Conclusions and outlook

In conclusion, we have presented a systematic study of the effects of small and large scale misalignment of GaAs and GaAs(Sb) SAG NWs with respect to the in-plane orientations on GaAs(2 1 1)B. We find that a 3° misaligned NW leads to ≈300% increase in the volume due to growth dynamics governed by adatom diffusion lengths and orientation dependent facet formation. The in-plane mis-orientation in defining trench openings within the substrate which leads to an undesired increase in facet roughness (S_q) of the NWs is important to be minimized in order to reduce structural disorder. We show that previously demonstrated use of Sb as a surfactant for NWs grown on standard (1 0 0) substrates also minimizes S_q for large scale misalignment, however it is not enough to obtain step-free [1 $\bar{1}$ $\bar{1}$]-oriented NWs on GaAs(2 1 1)B. Small scale misalignment is important to be considered for device design, in particular in light of the inherent errors associated with the tolerance of substrate manufacturing and fabrication. We estimate a length scale for which NWs can tolerate a certain degree of misalignment and suppress step formation. This means that AFM characterization of SAG NWs from a particular substrate prior to device fabrication can enable control over the crystal quality of the conducting channel by design. By virtue of the scalability of SAG, it can also be possible to make copies of the mask design for a range of in-plane orientations with $\theta = \pm 0.01°$, $\pm 0.02°$.. such that one of the NWs is bound to be perfectly aligned. Thus, for experiments with strict requirements on the magnitude of disorder in the semiconducting NWs, taking into account effects of misalignment on the NW morphology, careful design of the SAG mask and structural characterization of NWs prior to device fabrication should enable control of the NW crystal quality.

Author contribution statement

G N fabricated the SAG substrate, performed the MBE growth, acquired the AFM data. All authors contributed to data analysis and writing the manuscript.

Acknowledgments

This project has received funding from the European Research Council (ERC) under the European Union's Horizon 2020 research and innovation programme (Grant agreement no. 716655) and Microsoft Quantum. T S J acknowledges support from the ERC grant agreement no. 866158. G N would like to thank Peter Krogstrup, Anna Wulff Christensen, Tobias Særkjær and Steffen Zelzer for fruitful discussions. The authors acknowledge technical support from Claus Sørensen and Martin Bjergfelt. The Center for Quantum Devices is supported by the Danish National Research Foundation.

Data availability statement

All data that support the findings of this study are included within the article (and any supplementary files).

Conflict of interests

The authors declare no competing interests.

ORCID iDs

G Nagda https://orcid.org/0000-0001-7199-2033
T S Jespersen https://orcid.org/0000-0002-7879-976X

References

[1] Yuan X, Pan D, Zhou Y, Zhang X, Peng K, Zhao B, Deng M, He J, Tan H H and Jagadish C 2021 *Appl. Phys. Rev.* **8** 021302
[2] Krizek F *et al* 2018 *Phys. Rev. Mater.* **2** 093401
[3] Lee J S *et al* 2019 *Phys. Rev. Mater.* **3** 084606
[4] Beznasyuk D V *et al* 2022 *Phys. Rev. Mater.* **6** 034602
[5] Cachaza M E, Christensen A W, Beznasyuk D, Særkjær T, Madsen M H, Tanta R, Nagda G, Schuwalow S and Krogstrup P 2021 *Phys. Rev. Mater.* **5** 094601
[6] Ishitani A, Kitajima H, Endo N and Kasai N 1985 *Jpn. J. Appl. Phys.* **24** 1267
[7] Yamada T Y T and Horikoshi Y H Y 1994 *Jpn. J. Appl. Phys.* **33** L1027
[8] Kuriyama H K H, Ito M I M, Suzuki K S K and Horikoshi Y H Y 2000 *Jpn. J. Appl. Phys.* **39** 2457
[9] Tamai I, Sato T and Hasegawa H 2005 *Jpn. J. Appl. Phys.* **44** 2652
[10] Sato T, Tamai I and Hasegawa H 2005 Journal of Vacuum Science & Technology B: Microelectronics and Nanometer Structures Processing *Meas., Phenom.* **23** 1706
[11] Albani M, Ghisalberti L, Bergamaschini R, Friedl M, Salvalaglio M, Voigt A, Montalenti F, Tütüncüoglu G, Fontcuberta i Morral A and Miglio L 2018 *Phys. Rev. Mater.* **2** 093404
[12] Wang N, Yuan X, Zhang X, Gao Q, Zhao B, Li L, Lockrey M, Tan H H, Jagadish C and Caroff P 2019 *ACS Nano* **13** 7261
[13] Borg M *et al* 2018 *Nanotechnology* **30** 084004
[14] Desplanque L, Fahed M, Han X, Chinni V K, Troadec D, Chauvat M-P, Ruterana P and Wallart X 2014 *Nanotechnology* **25** 465302
[15] Zeng L, Gammer C, Ozdol B, Nordqvist T, NygÅrd J, Krogstrup P, Minor A M, Jäger W and Olsson E 2018 *Nano Lett.* **18** 4949
[16] E-Beam Resist AR-P 6200 series (CSAR 62) - Allresist EN, (2021), [Online; accessed 31. May 2022] (https://allresist.com/wp-content/uploads/sites/2/2020/03/AR-P6200_CSAR62english_Allresist_product-information.pdf)
[17] Aseev P *et al* 2019 *Nano Lett.* **19** 218
[18] Markov I and Stoyanov S 1987 *Contemp. Phys.* **28** 267
[19] Quirk M and Serda J 2001 *Semiconductor Manufacturing Technology* (Upper Saddle River, NJ, Columbus, OH: Prentice Hall)
[20] Markov I 1999 *Surf. Sci.* **429** 102
[21] Nomura Y, Morishita Y, Goto S, Katayama Y and Isu T 1994 *Appl. Phys. Lett.* **64** 1123
[22] Einstein T L 2015 *Handbook of Crystal Growth* 2nd edn (Walthm, MA: Elsevier) vol 1, p 215
[23] Yeu I W, Han G, Park J, Hwang C S and Choi J-H 2019 *Sci. Rep.* **9** 1
[24] Markov I V 2017 *Crystal Growth for Beginners* 2nd edn p 493
[25] Fong C Y, Watson M D, Yang L H and Ciraci S 2002 *Model. Simul. Mater. Sci. Eng.* **10** R61